European Journal of Neuroscience, Vol. 27, pp. 580–592, 2008 doi:10.1111/j.1460-9568.2008.06040.x

Tyrosine hydroxylase cells appearing in the mouse striatum after dopamine denervation are likely to be projection neurones regulated by L-DOPA

Sanja Darmopil,[1,2] Vilma C. Muñetón-Gómez,[1,2] María L. de Ceballos,[1,2] Miya Bernson[1] and Rosario Moratalla[1,2]
[1]Cajal Institute, Consejo Superior de Investigaciones Científicas, Avda Dr Arce 37, 28002 Madrid, Spain and
[2]CIBERNED, Instituto de Salud Carlos III, Madrid, Spain

Keywords: aromatic-L-amino acid decarboxylase, dopamine transporter, L-3, 4-dihydroxyphenylalanine, neurogenesis, Parkinson's disease

Abstract

Tyrosine hydroxylase (TH)-immunoreactive (ir) neurones are detected in the striatum of animals after dopamine depletion and also in human parkinsonian patients. Although there is extensive evidence for TH-ir neurones in the lesioned rodent striatum, there are few details regarding the molecular phenotype of these neurones, regulation of their TH expression after L-3,4-dihydroxyphenylalanine (L-DOPA) treatment and their function. In the present study, we examined the time-course of appearance of TH-ir neurones in the mouse striatum after 6-hydroxydopamine (6-OHDA) lesion and determined their molecular phenotype. We found that TH-ir neurones appeared in the striatum as early as 3 days after a 6-OHDA lesion. By 1 week after the lesion, the number of TH-ir neurones started to decrease and this decrease progressed significantly over time. Treatment with L-DOPA increased both the number of TH-ir neurones and the intensity of their immunolabelling. The TH-ir neurones that appear after the 6-OHDA lesion in the striatum are not newly generated cells as they did not incorporate 5-bromo-2-deoxyuridine. We found that the vast majority of TH-ir neurones colocalized with dynorphin and enkephalin, suggesting that they are projection neurones of the direct and indirect striatal output pathways. TH-ir neurones did not express the dopamine transporter but half of them expressed amino acid decarboxylase, an enzyme required for dopamine synthesis. Finally, striatal TH-ir neurones are functionally active, expressing the neuronal activation marker FosB in response to L-DOPA treatment. Promotion of these striatal TH-ir neurones may be beneficial in Parkinson's disease, particularly in the early stages when dopamine denervation is incomplete.

Introduction

The principal pathological feature of Parkinson's disease is loss of neurones in the substantia nigra pars compacta leading to a deficiency in striatal dopamine that is responsible for the major symptoms of the disease. Despite advances in Parkinson's disease research, current treatments target symptomatic relief and administration of L-3, 4-dihydroxyphenylalanine (L-DOPA) to replace lost dopamine is still the most effective therapy available. Convincing evidence has emerged from animal and human studies that additional dopaminergic neurones exist in the striatum itself (Huot & Parent, 2007) and that the number of these neurones varies in parkinsonian patients (Porritt *et al.*, 2000; Huot *et al.*, 2007). These findings have implications for a new approach to Parkinson's disease therapy. However, the origin and molecular phenotype of these neurones and their potential physiological role remain to be defined.

Projection neurones constitute over 90% of the striatal neuronal population (DiFiglia *et al.*, 1976; Chang *et al.*, 1982). These projection neurones are GABAergic, express calbindin and can be further subdivided into two populations (Kawaguchi *et al.*, 1990): direct pathway neurones, which express substance P and dynorphin, and indirect pathway neurones, which express enkephalin. The interneuronal population is comprised of cholinergic interneurones, identified by the presence of choline acetyltransferase, and GABAergic interneurones divided according to their neuropeptide content (parvalbumin, calretinin and somatostatin) (Kawaguchi *et al.*, 1995). More recently, another neuronal population has been described in the adult rodent and primate striatum, characterized by the expression of tyrosine hydroxylase (TH). These neurones were first reported in the rat striatum by Tashiro *et al.* (1989) and later on by other groups (Lopez-Real *et al.*, 2003; Jollivet *et al.*, 2004). The number of these neurones increases following 6-hydroxydopamine (6-OHDA) lesion (Mura *et al.*, 1995; Betarbet *et al.*, 1997; Lopez-Real *et al.*, 2003; Jollivet *et al.*, 2004).

Striatal TH-immunoreactive (ir) neurones have been shown to coexpress the glutamic acid decarboxylase$_{67}$ isoform of glutamic acid decarboxylase, a key enzyme in GABA production (Betarbet *et al.*, 1997; Tande *et al.*, 2006) that intensely stains striatal interneurones (Mercugliano *et al.*, 1992). Lack of calbindin expression (Cossette *et al.*, 2005b; Tande *et al.*, 2006) also suggests that these TH-ir cells are interneurones (Gerfen *et al.*, 1985). In addition, in humans and other primates, striatal TH-ir neurones express the nuclear transcription factor Nurr1, known to maintain the dopaminergic phenotype (Cossette *et al.*, 2004, 2005b) and the dopamine transporter (DAT) (Porritt *et al.*, 2000; Cossette *et al.*, 2005b; Tande *et al.*, 2006; Huot *et al.*, 2007; San Sebastian *et al.*, 2007), suggesting that they have a dopaminergic phenotype. As the adult striatum can generate new

Correspondence: Dr Rosario Moratalla, [1]Cajal Institute, as above.
E-mail: moratalla@cajal.csic.es

Received 11 May 2007, revised 28 November 2007, accepted 10 December 2007

neurones (Bedard *et al.*, 2002), it is possible that the appearance of TH-ir cells in the dopamine-depleted striatum is due either to *de-novo* generation or to a phenotype induction in a subpopulation of pre-existing striatal neurones.

This study characterizes striatal TH-ir neurones in hemiparkinsonian mice. We studied the time-course of appearance, origin and molecular phenotype of striatal TH-ir neurones after unilateral 6-OHDA lesion, as well as activation of these cells by a dopaminergic stimulus.

Materials and methods

Animals

Adult male C57/BL6 mice (Cajal Institute, Consejo Superior de Investigaciones Científicas, Madrid, Spain) were housed in standard Plexiglas cages with a maximum of six animals per cage and *ad-libitum* access to food and water. The environmental conditions were strictly controlled with a 12 h light/dark cycle, a temperature of 22 °C and 44% humidity. All animal maintenance and experimental procedures were in accordance with the guidelines laid out in the European Union Council Directive (86/609/EEC). All efforts were made to minimize the number of animals used in this study. The experimental protocols involving animals were approved by the Consejo Superior de Investigaciones Científicas ethics committee.

Striatal unilateral 6-OHDA lesion

Mice were anaesthetized with an intraperitoneal injection of 200 mg/kg of 2,2,2-tribromoethanol (Sigma-Aldrich) and placed in a stereotaxic frame with a mouse adapter (David Kopf Instruments, Tujunga, CA, USA). Antibiotic cream was used to protect the eyes from drying during surgery. At 30 min before lesion, the mice received an intraperitoneal injection of 20 mg/kg of the noradrenaline reuptake inhibitor desipramine hydrochloride (Sigma-Aldrich) to protect the noradrenergic neurones from 6-OHDA neurotoxicity (Breese & Traylor, 1971).

Using a Hamilton syringe (Hamilton, Bonaduz, Switzerland), 4 μL of 6-OHDA-HBr solution (10 mM) in 0.1% ascorbic acid (Sigma-Aldrich) was injected in the left striatum at the following stereotaxic coordinates in two deposits (Paxinos & Franklin, 2004): AP, 0.65; L, 2.0; V_1, −4 and V_2, −3 mm.

After the injection, the skin was sutured and the animals were removed from the stereotaxic instrument and placed on a heating pad for 30 min. During the first days after surgery animals received injections of saline solution to prevent dehydration, as well as supplementary food.

BrdU injections

To identify mitotic cells, adult male mice received two intraperitoneal injections of 5-bromo-2-deoxyuridine (BrdU) (Sigma-Aldrich) at a dose of 50 mg/kg (diluted in saline). Injections were administered 12 h apart, starting 24 h ($n = 3$) or 48 h ($n = 3$) after the 6-OHDA lesion. The animals were killed at 24 h after the last BrdU injection. Additionally and in order to follow the time-course of the appearance of TH-ir neurones in the striatum, six adult male mice were killed at 1 ($n = 3$) or 2 weeks ($n = 3$) after the lesion.

L-DOPA treatment

To evaluate whether L-DOPA modulates the appearance of TH-ir striatal neurones, a group of 12 mice were lesioned with 6-OHDA. These animals were divided into two experimental groups of six mice each at 4 weeks after the lesion and subjected to treatment with L-DOPA methyl ester (Sigma-Aldrich) or saline for 3 weeks. During this treatment period, the animals received daily intraperitoneal injections of 6 mg/kg benserazide hydrochloride (Sigma-Aldrich), a peripheral blocker of L-DOPA decarboxylase, and 20 min later an injection of 15 mg/kg of L-DOPA. Control animals received a single saline injection of the corresponding volume.

Tissue preparation

Adult animals were killed with an overdose of pentobarbital (Laboratorios Normon, Madrid, Spain) and were injected intracardially with 0.5 mL of 1% heparin (Rovi, Madrid, Spain), which was followed by the perfusion of 10 mL of saline and 100 mL of 4% paraformaldehyde, pH 7.4. Animals that received L-DOPA were killed at 1 h after the last L-DOPA injection. The brains were post-fixed for 24 h and were then transferred to a solution of 0.1 M phosphate buffer containing 0.02% sodium azide for storage at 4 °C. To obtain regular blocks, brains were further immersed in 3% agarose and cut at a thickness of 40 μm using a vibratome (Leica, Wetzlar, Germany).

Immunohistochemistry and western blot experiments

Immunostaining was carried out in free-floating sections using a standard avidin–biotin immunocytochemical protocol (Rivera *et al.*, 2002; Grande *et al.*, 2004). Endogenous peroxidase activity was quenched by incubation for 10 min in 0.1 M phosphate-buffered saline containing 0.2% Triton X-100 with 3% hydrogen peroxide. Non-specific binding sites were blocked for 60–90 min with 5–10% of the appropriate serum in phosphate-buffered saline containing 0.2% Triton X-100. To localize TH-ir neurones we used rabbit TH antisera (1 : 1000; Chemicon, Temecula, CA, USA) and a monoclonal TH antibody (1 : 250; ImmunoStar, Hudson, WI, USA). The specificity of the two antibodies against TH protein was assessed by western blotting. Protein extracts from the striata and liver of two C57/BL6 adult male mice were prepared as described (Grande *et al.*, 2004) and 40 μg of each extract was resolved by sodium dodecyl sulphate polyacrylamide gel electrophoresis and blotted onto a nitrocellulose membrane. Immunodetection was carried out with both TH antibodies at a concentration of 1 : 250. Bands were visualized by enhanced chemiluminescence (Amersham, Buckinghamshire, UK) and films were scanned to obtain photographs (Quantity One, Bio-Rad, Madrid, Spain). Both antibodies recognized a single band around 60 kDa in the striatal samples. No band was detected in the protein extracts taken from the liver of the same animals, used here as negative control. These results indicate that both antibodies are specific for TH and detect an identical protein (Fig. 1).

To visualize BrdU incorporation and examine the possible neurogenesis of TH-ir neurones in the lesioned striatum, we used a biotinylated BrdU sheep antiserum (1 : 100; Abcam, Cambridge,

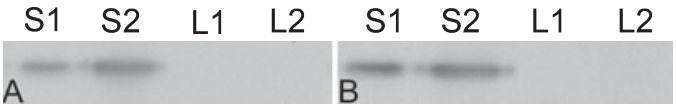

FIG. 1. Antibodies used in the study are specific for TH. Western blot assay of striatum (S1 and S2) and liver (L1 and L2) samples using (A) polyclonal anti-TH rabbit antiserum and (B) monoclonal TH antibody. Both antibodies recognize a single TH-ir band at approximately 60 kDa in striatal samples. Liver samples did not show any TH immunoreactivity. Each experiment was performed at least three times with similar results, $n = 2$ animals.

UK), as well as a guinea pig doublecortin antiserum (1 : 3000; Chemicon) that labels migrating neurones and a rabbit nestin antiserum (McManus *et al.*, 1999) as a marker of neuroepithelial stem cells or immature cells. To identify striatal projection neurones, we used a rabbit Dynorphin B antiserum for the neurones of the direct pathway (1 : 10 000; Serotec Ltd, Oxford, UK), a rabbit met-enkephalin antiserum for the neurones of the indirect pathway (1 : 500; Instar, Stillwater, MN, USA) and a rabbit calbindin antiserum (1 : 250; Moratalla *et al.*, 1996). To identify striatal interneurones, a goat antiserum choline acetyltransferase (1 : 500; Chemicon) was used to label cholinergic interneurones, as well as a monoclonal mouse antibody against parvalbumin (1 : 500; Sigma), a monoclonal rat antibody against somatostatin (1 : 100) (Milstein & Cuello, 1983) and a goat calretinin antiserum (1 : 1000; Chemicon). Neuronal activation was visualized using a rabbit FosB antiserum (1 : 10 000; Santa Cruz Biotechnology, Santa Cruz, CA, USA) (Pavon *et al.*, 2006). To assess the dopaminergic phenotype we used a rat monoclonal antibody against DAT (1 : 1000; Chemicon) and rabbit aromatic-L-amino acid decarboxylase (AADC) antisera (1 : 250; Chemicon or Abcam).

With the exception of anti-enkephalin and anti-DAT, all primary antibodies were diluted in 0.1 M phosphate-buffered saline containing 0.2% Triton X-100 and 1% serum of the animal in which the secondary antibody was produced. Anti-enkephalin was diluted in 0.1 M phosphate-buffered saline and 1% of the appropriate serum but without Triton X-100. The anti-DAT antibody was prepared using 0.1 M Tris-buffered saline with 0.2% Triton X-100. To obtain anti-BrdU staining it was necessary to denature the DNA after blocking peroxidase activity. DNA denaturation was performed by incubating sections in 1 M HCl solution on ice for 10 min, then in 2 M HCl for 10 min at room temperature (24 °C) and finally for 20 min at 37 °C. HCl was neutralized with 0.1 M sodium borate for 10 min. For immunohistochemistry with monoclonal antibodies on mouse sections, we used a mouse-on-mouse Vecstatin kit (Vector Laboratories, Burlingame, CA, USA) to block mouse IgGs in the tissue according to the manufacturer's instructions.

After incubation with the primary antibody (usually overnight), the sections were washed and incubated with the appropriate biotinylated secondary antibody (1 : 500) (all from Vector Laboratories) for 1–2 h at room temperature. After washing, the sections were incubated with streptavidin (Zymed, San Francisco, CA, USA) for 1 h and antibody staining was developed using DAB (Sigma-Aldrich). After developing the reaction, stained sections were mounted, dried, dehydrated, coverslipped with Permount mounting medium (Fisher Chemicals, Fair Lawn, NJ, USA) and examined using a light microscope (Leica, Heidelberg, Germany).

Double-labelling fluorescent immunohistochemistry was performed following a similar protocol. Sections were incubated for 2 h at room temperature with the appropriate Alexa-conjugated (all from Molecular Probes, Invitrogen, Eugene, OR, USA) or biotinylated secondary antibodies, followed by incubation with fluorescent Alexa-conjugated horseradish streptavidin for 1 h (Molecular Probes). Sections were mounted in fluorescent mounting medium (DABCO, Fluka, Buchs, Switzerland), coverslipped and kept in the dark at 4 °C until they were examined by laser confocal microscopy (Leica). The specific immunofluorescence of the Alexa 488 or Alexa 568/594 fluorophores was visualized by excitation at 488 or 568 nm, respectively.

Cellular density: TH-ir neurone and fibre quantification and statistical analysis

The quantification of TH-ir neurones in the striatum of 6-OHDA-lesioned animals and animals treated with L-DOPA after inducing the 6-OHDA lesion was measured in five to six coronal sections per animal using Neurolucida software (Microbrightfield, Colchester, VT, USA). The borders of the areas of interest were outlined from a live image with a 4× objective and the entire area of interest was examined using a 20× objective. Only TH-ir cells with an identifiable unlabelled nucleus surrounded by TH-immunolabelled cytoplasm or those with labelled dendrites were counted. The images were then exported to Neuroexplorer (Microbrightfield) to determine the cross-sectional area of the striatum and the relative density of TH-ir neurones. Data were expressed as the number of TH-ir neurones per mm^2 of striatum per animal. We analysed six animals per group with the exception of the animals killed at 1 ($n = 3$) and 2 ($n = 3$) weeks post-lesion.

Quantification of TH-ir fibres was carried out by optical density analysis (Granado *et al.*, 2008), with the aid of an image analysis system (AIS, Imaging Research Inc., Linton, UK) using a 40× lens. TH-ir fibre staining intensity was determined in striatal areas surrounding TH-ir neurones, through the rostrocaudal extent of the dopaminergic lesion. Similar measurements were carried out in the unlesioned striatum in randomly chosen areas. The data from the lesioned side are presented as a percentage (mean ± SE) of the values from the unlesioned striatum. Measurements were carried out in striatal sections from five denervated animals treated with L-DOPA (four to five sections per animal).

Statistical analysis was performed using one-way ANOVA and Student-Newman-Keuls post-hoc test. The threshold for statistical significance was set at $P < 0.05$.

Results

TH-ir neurones in the denervated mouse striatum: time-course of appearance, morphology, distribution and modulation by L-DOPA treatment

Following 6-OHDA lesion, immunohistochemistry revealed TH-ir cells in the denervated striatum but not in the unlesioned side. Examination under light microscopy revealed that most of these neurones had an oval or rounded soma of 8–15 μm in diameter (12 μm on average). Some exhibited a more elongated (bipolar) soma with diameters around 17 μm in the longest axis and 10 μm in the shortest axis. The majority had two to four primary dendrites arising from the neuronal soma (Fig. 2).

To establish the time-course of appearance of TH-ir neurones after lesion, we examined striatal coronal sections from animals killed at 0.5, 1, 2 and 7 weeks after 6-OHDA lesion. Dopaminergic denervation with 6-OHDA produces a rapid loss of striatal dopamine fibres around the injection site, evident at 24 h after injection of the neurotoxin (Jollivet *et al.*, 2004). TH-ir neurones were observed in the lesioned striatum as early as 3 days (0.5 weeks) after the lesion (Fig. 2A and G) and at all post-lesion periods examined (up to 7 weeks; Fig. 2). The intensity of TH staining in these neurones was highest at 0.5 weeks after the lesion and decreased over time. In the striatum of animals killed at 0.5–2 weeks after the 6-OHDA administration, TH immunoreactivity was mainly observed in the cytoplasm of the neuronal soma, and was also occasionally present in the dendrites, but dendritic spines were rarely visualized with TH immunoreactivity (Fig. 2A–C). We did not observe TH-ir cells in the non-lesioned side of the striatum at any time-point.

To study the effect of L-DOPA on TH-ir striatal neurones, lesioned animals were treated daily with 15 mg/kg of L-DOPA for 3 weeks, beginning at the 4th week after the lesion. Control animals received saline instead of L-DOPA. At 7 weeks post-lesion, most of the striatal

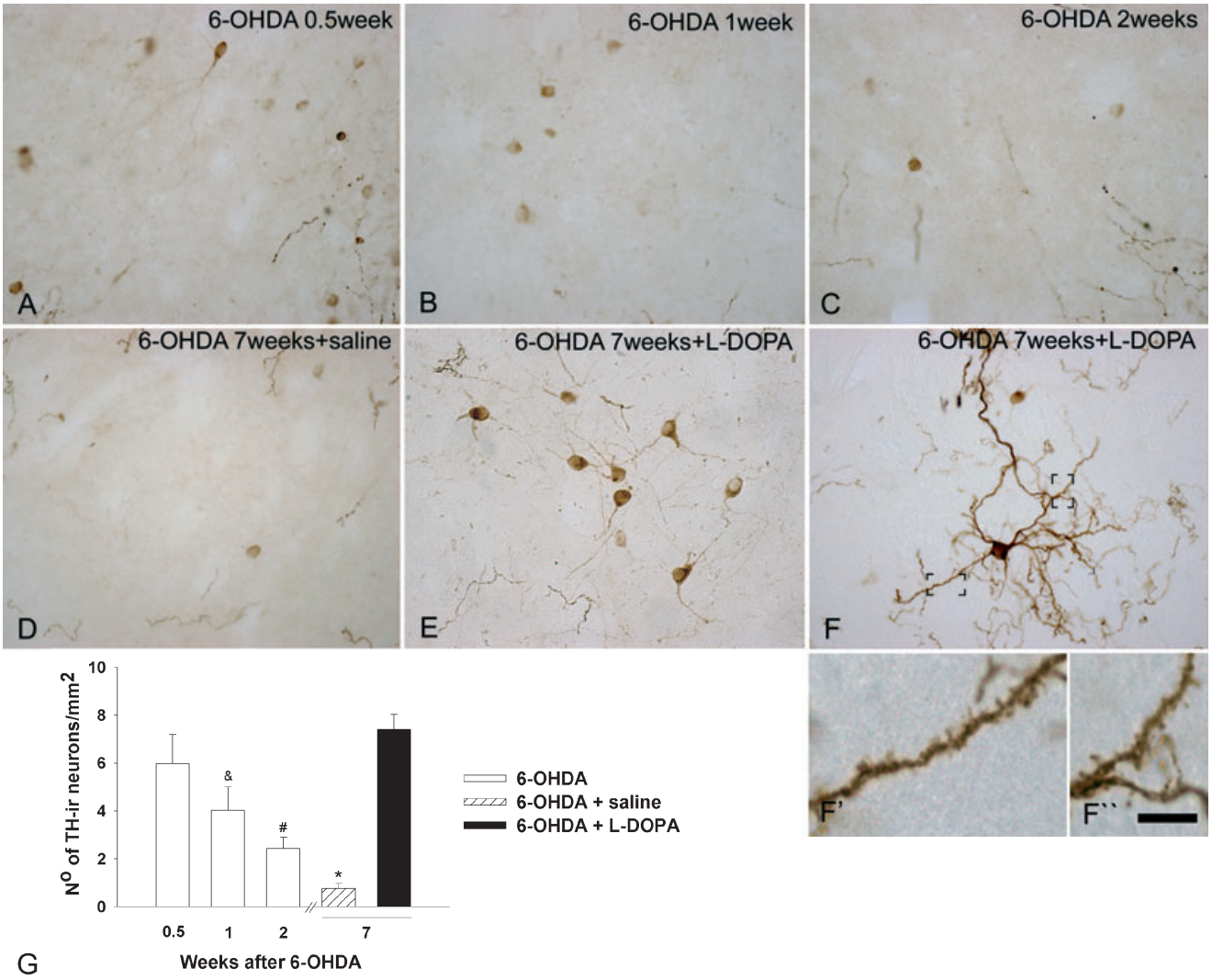

FIG. 2. Time-course of the appearance and cellular density of TH-ir neurones in the mouse striatum following 6-OHDA lesion and L-DOPA treatment. Micrographs of TH-ir neurones in the mouse striatum at different time-points after 6-OHDA lesion without (A–D) or with (E and F) L-DOPA treatment. Note the increase in the intensity of TH immunostaining of the neurone soma and the labelling of dendrites in the striatum of L-DOPA-treated animals compared with controls. (F′ and F″) High magnification of dendrite segments (in boxes) from the neurone in F illustrating numerous dendritic spines. Scale bars: 50 μm (A–F); 6 μm (F′ and F″). (G) Histograms indicate the density of TH-ir neurones (mean + SE) in the striatum after 6-OHDA lesion and L-DOPA treatment. $^{*}P < 0.001$ vs. L-DOPA-treated animals and animals killed at 0.5 week after 6-OHDA lesion; $^{\#}P < 0.01$ vs. L-DOPA-treated animals and animals killed at 0.5 week after 6-OHDA lesion; $^{\&}P < 0.05$ vs. L-DOPA-treated animals ($n = 3$–6).

TH-ir neurones observed in saline control animals displayed weak immunoreactivity in the soma (Fig. 2D). Dendrites were observed in only a few cells (one to three per brain section). These cells were always localized close to the spared TH fibres. By contrast, treatment with L-DOPA markedly increased both the number and labelling intensity of TH-ir neurones in the lesioned striatum when compared with lesioned animals treated with saline (Fig. 2D and E) or with animals killed at shorter post-lesion times (Fig. 2A–C). The morphology of the TH-ir neurones in the lesioned striatum of L-DOPA-treated animals corresponded to that seen in the absence of L-DOPA (described above) but there was generally more complete labelling of the dendritic tree (Fig. 2E and F). In almost all cases, primary dendrites were evident, secondary dendrites were found less frequently (Fig. 2E) and, in a few cases, dendritic spines were observed (Fig. 2F, F′ and F″).

To confirm that there were no TH-ir cells in the unlesioned side of the striatum, we examined TH immunofluorescence in the striatum with confocal microscopy using serial z-axis planes (2 μm apart) through the thickness of the section. Microphotographs of both 6-OHDA-lesioned striatum and the unlesioned side in a mouse treated with L-DOPA are provided as supplementary material (supplementary Fig. 1). These ultrafine planes show thin layers of nigrostriatal fibres in the unlesioned side and no TH-ir soma. TH-ir cells are clearly evident in the lesioned side of the striatum and it appears that detection is strong enough that any TH-ir cells in unlesioned striatum should be visible above the background of TH-ir fibres. Our results are in agreement with previous reports showing no TH-expressing soma in unlesioned striatum (Jaber *et al.*, 1999; Baker *et al.*, 2003).

In general, the distribution of TH-ir neurones in the striatum corresponded with the location of spared dopaminergic fibres after the 6-OHDA lesion. However, TH-ir neurones could be observed throughout the whole rostrocaudal extent of the striatum if local dopamine depletion was greater than 95%. In lesioned animals treated with saline observed at 7 weeks after the lesion, these neurones were most frequently found in the ventral striatum close to the spared TH fibres (Fig. 3B). The distribution of TH-ir neurones in the striatum of

L-DOPA-treated animals followed a similar rostrocaudal pattern; however, they were more numerous, especially in the dorso-lateral portion of striatum, in almost completely denervated areas (Figs 3A and A′, and 4).

We quantified the remaining dopaminergic fibres in the area immediately surrounding the TH-ir neurones and found that TH-ir neurones were present in striatal areas with a TH fibre content of 1.99 ± 0.96% of unlesioned values (Fig. 4C and D). Very few TH-ir neurones were found in areas with lower (Fig. 4B) or higher (Fig. 4E–G) TH fibre content. This is quite interesting because it indicates that proximity to spared dopaminergic terminals is required for L-DOPA-induced neuronal TH expression. Spared dopaminergic terminals are not sufficient to induce TH expression in neurones in the lesioned striatum as saline treatment does not increase TH expression in striatal neurones.

Cellular density of TH-ir neurones in the 6-OHDA-lesioned striatum: modulation by L-DOPA

We next examined changes in the density of striatal TH-ir neurones, quantifying these neurones at different times after the 6-OHDA lesion and after L-DOPA treatment. Cell counting was performed using a light microscope coupled to the Neurolucida system. We found a considerable number of striatal TH-ir neurones at 0.5 weeks after the lesion (6.0 ± 1.2 neurones/mm^2). The number of TH-ir neurones decreased with time to 2.4 ± 0.5 TH-ir neurones/mm^2 at 2 weeks and to 0.8 ± 0.2 neurones/mm^2 at 7 weeks after the lesion. Daily L-DOPA treatment beginning in the 4th week post-lesion increased the density of TH-ir neurones in the lesioned striatum at 7 weeks post-lesion to 7.4 ± 0.7 neurones/mm^2. This is statistically greater than the numbers of TH-ir neurones in animals killed at 1 ($P < 0.05$) and 2 ($P < 0.01$) weeks after the lesion and significantly greater than control lesioned animals treated with saline and killed at 7 weeks post-lesion ($P < 0.001$, Fig. 2G).

BrdU incorporation

To determine whether striatal cells expressing TH were generated *de novo* after dopamine lesion, mice were administered 50 mg/kg BrdU in two separate injections 12 h apart, starting 24 or 48 h after the administration of 6-OHDA. These time-points were selected as the greatest expression of TH (in terms of label intensity and number of labelled cells) was observed in the middle of the 1st week after the lesion. We found numerous BrdU-ir cells in the lesioned striatum of mice killed at 0.5 or 1 week after lesion. BrdU-ir cells were distributed homogeneously in the striatum, many of them emerging in pairs (Fig. 5B); however, BrdU labelling never colocalized with TH (Fig. 5). In addition, we performed immunostaining for doublecortin, which can be found in migrating and differentiating neurones, as well as for nestin, an intermediate filament protein that labels dividing and migrating cells. We found no doublecortin-immunolabelled cells in the lesioned striatum but there was prominent nestin immunolabelling, suggesting strong gliosis throughout the lesioned striatum (data not shown). In summary, using BrdU, nestin and doublecortin immunostaining we were unable to identify newborn TH-ir neurones after administration of 6-OHDA in the mouse striatum.

Phenotypic characterization of striatal TH-ir neurones

On the basis of these results, we set out to study the molecular phenotype of the TH-ir neurones observed in the dopamine-depleted striatum of mice, to see whether they correspond to any of the known striatal cell types or to a new class of striatal neurones. Phenotypic characterization was performed in striatal sections from 6-OHDA-lesioned mice treated with either saline or L-DOPA. Qualitative studies yielded similar results in both groups of animals. However, due to the very low number of TH-ir neurones in the striata of lesioned/saline-treated animals we did not quantify the results in this group.

We carried out double fluorescent immunohistochemistry to determine whether TH colocalized with calbindin (a marker of projection neurones), dynorphin (a marker for direct pathway projection neurones) or enkephalin (a marker for indirect pathway projection neurones). Quantification under confocal microscopy demonstrated that 54% of striatal TH-ir neurones also expressed dynorphin (Fig. 6A–C), 45% also expressed enkephalin (Fig. 6D–F) and 80% of TH-ir neurones expressed calbindin (Fig. 6G–I). These results indicate that the vast majority of these striatal TH-ir neurones are striatal projection neurones, including both direct and indirect pathway neurones.

We also studied whether striatal TH-ir neurones express any of the specific markers for the different interneurone types in the striatum, using antibodies specific for choline acetyltransferase, parvalbumin, somatostatin or calretinin, markers of the four main striatal interneurone types described. We did not find any colocalization of TH with choline acetyltransferase, parvalbumin or somatostatin (Fig. 7). However, we did find that some TH-ir neurones express calretinin (Fig. 7J–L). Quantification showed that about 1% of the TH-ir neurones examined expressed calretinin. Interestingly, in the present study as well as in a previous study (Mura *et al.*, 2000), calretinin-ir neurones were more numerous in the dopamine-depleted than in the intact striatum. These calretinin- and TH-ir neurones had a smaller cell body than the other TH-ir neurones and the intensity of calretinin labelling in these cells was weaker than in calretinin-ir neurones that did not coexpress TH. Moreover, TH/calretinin-ir neurones were usually localized in the rostral sections of the medial striatum and close to the shell of the nucleus accumbens.

We also examined expression of the DAT, which is responsible for the reuptake of dopamine. DAT immunoreactivity was present in the spared dopamine fibres in the lesioned striatum, where it colocalized with TH (Fig. 8C, arrows). However, DAT immunoreactivity was not observed in the striatal TH-ir neurones or in any cell soma in the mouse striatum (see Fig. 8A–C, arrowhead).

The potential of striatal TH-ir neurones to produce dopamine was assessed by studying expression of AADC, the enzyme responsible for the conversion of L-DOPA to dopamine. In the 6-OHDA-lesioned striatum the number and intensity of AADC-ir fibres decreased to a similar extent as TH-ir fibres did and then the appearance of striatal AADC-ir cell somas was also evident. These striatal AADC-positive neurones were primarily distributed along the dorsal part, below the corpus callosum, but were also found around spared AADC-ir fibres and in the ventral striatum where the lesion is less effective. About half of the AADC-ir neurones observed in the lesioned striatum were of small diameter (6–10 μm) (Fig. 8E′ and F′) and the rest were of a larger diameter (10–15 μm). We found that around half of the TH-ir neurones in the striatum also expressed AADC and that neurones that expressed both markers belonged to the larger type of AADC neurones (Fig. 8D–F).

Functional activation of striatal TH-ir neurones

In order to verify whether these striatal TH-ir neurones are able to respond to L-DOPA, we assessed the expression of the transcription

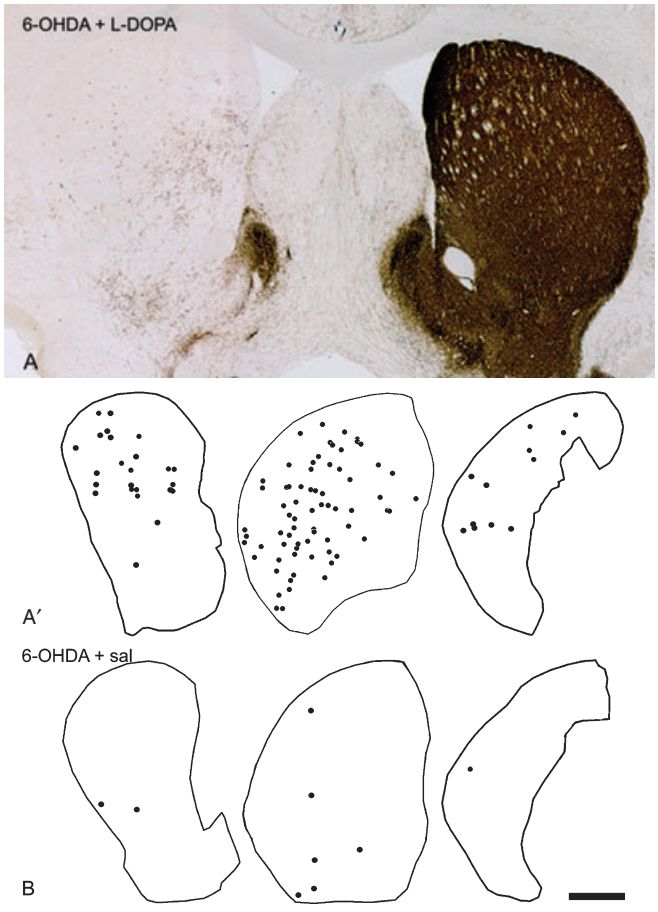

FIG. 3. Distribution of TH-ir neurones in the mouse striatum following 6-OHDA lesion and L-DOPA treatment. (A) Photomicrograph showing TH immunostaining in coronal brain sections from a representative animal with unilateral 6-OHDA lesion treated with L-DOPA (15 mg/kg), beginning at 4 weeks post-lesion and continuing for 3 weeks before killing. (A′ and B) Neurolucida drawings of dopamine-depleted striatum at three different rostro-caudal levels showing the distribution of TH-ir neurones in a mouse treated with L-DOPA (15 mg/kg) for 3 weeks (A′) or with saline (sal) (B). Note in A that few dopaminergic fibres in the ventral portion of the striatum are spared, although the fibre density was much lower than in the non-lesioned, contralateral side. Scale bars: 500 μm (A); 750 μm (A′ and B).

factor FosB (a marker of neuronal activity) in these neurones using both immunofluorescence and DAB labelling. FosB expression has been shown to be induced in striatal projection neurones after dopaminergic stimulation (Moratalla *et al.*, 1996; Grande *et al.*, 2004; Pavon *et al.*, 2006). Stimulation with L-DOPA increases FosB expression in the dopamine-denervated striatum (Andersson *et al.*, 1999; Lundblad *et al.*, 2004; Pavon *et al.*, 2006). We also observed FosB expression in these striatal TH-ir neurones after L-DOPA administration. Most, if not all, of the striatal TH-ir neurones observed in the lesioned striatum (in completely denervated areas or near spared TH fibres) expressed FosB after L-DOPA treatment. Interestingly, whereas FosB, a transcription factor, is usually only expressed in the nucleus, in these striatal TH-ir neurones, FosB expression was present not only in the nucleus but also in the cytoplasm and primary dendrites (Fig. 8H and I, asterisk). These results indicate that these neurones are responsive to L-DOPA treatment and are therefore functionally active.

Discussion

The current study demonstrates that TH-ir neurones appear in the lesioned mouse striatum as soon as 3 days after 6-OHDA injection. However, after the 1st week post-lesion the number of TH-ir neurones begins to decrease and this decrease progresses over time. Treatment with L-DOPA increased both the number of TH-ir neurones and the intensity of their immunolabelling. The TH-ir neurones that appear after the 6-OHDA lesion in the striatum are not newly generated cells as they did not incorporate BrdU. We report for the first time that almost all of these striatal TH-ir neurones are projection neurones of the direct and indirect striatal output pathways, as demonstrated by the colocalization of TH with either dynorphin or enkephalin and with calbindin. Only 1% of TH-ir neurones expressed calretinin, a marker for a type of striatal interneurones. In the mouse striatum, TH-ir neurones did not express DAT but around half of these neurones expressed AADC, an enzyme involved in dopamine synthesis. Finally, TH-ir neurones were functionally active, expressing the neuronal activation marker FosB in response to L-DOPA treatment.

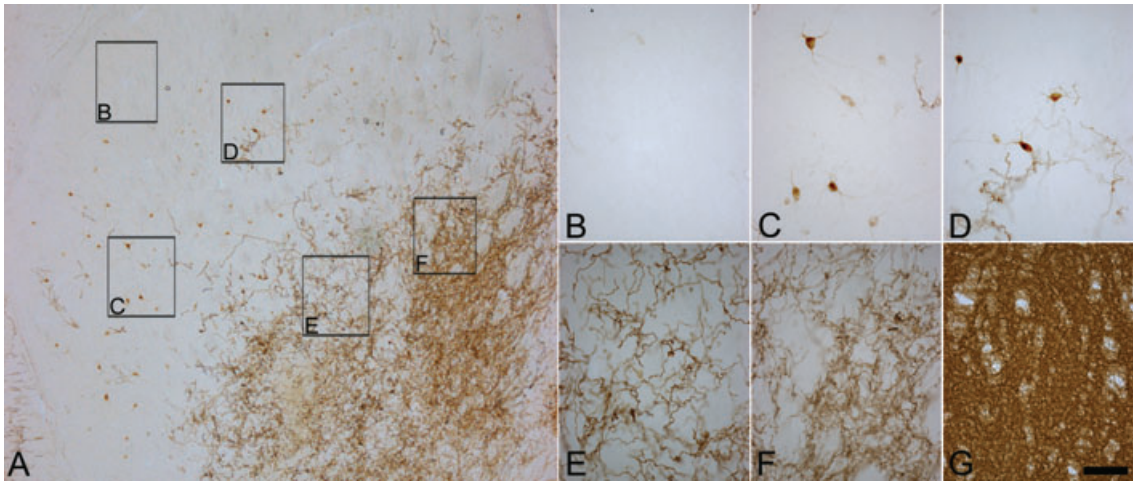

FIG. 4. Localization of TH-ir neurones in parts of striatum with different degrees of dopaminergic denervation. Photomicrographs showing TH immunolabelling of 6-OHDA-lesioned (A–F) and unlesioned striatum (G). Enlarged photomicrographs (B–F) illustrate the absence of TH-ir neurones in completely denervated areas (B) of the striatum and their presence in striatal regions with a few remaining dopaminergic fibres (C and D). We found no TH-ir neurones in partially lesioned striatal areas (E and F) or in the contralateral unlesioned striatum (G). Scale bars: 260 μm (A); 50 μm (B–F).

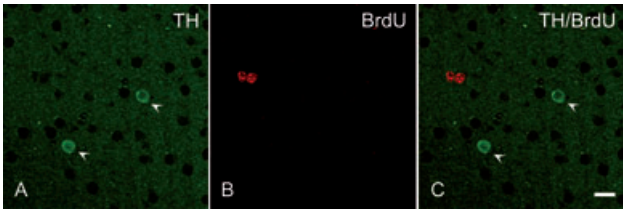

FIG. 5. TH-ir neurones in the mouse striatum following 6-OHDA lesion did not incorporate BrdU. Confocal laser photomicrographs from the striatum of a mouse that received BrdU injections at 24 h after 6-OHDA and was killed 2 days later, showing double immunostaining for TH (A) and BrdU (B). The two markers do not colocalize (C). Scale bar, 15 μm.

Time-course of appearance and distribution of striatal TH-ir neurones after 6-OHDA lesion and L-DOPA treatment

Although numerous studies have identified TH-ir neurones in normal and dopamine-depleted human (Porritt *et al.*, 2000; Cossette *et al.*, 2005a), monkey (Dubach *et al.*, 1987; Betarbet *et al.*, 1997; Mazloom & Smith, 2006; Tande *et al.*, 2006) and rat striatum (Tashiro *et al.*, 1989; Mura *et al.*, 1995; Meredith *et al.*, 1999; Lopez-Real *et al.*, 2003; Jollivet *et al.*, 2004), there are very few reports of TH-ir striatal neurones in mice. Previously, TH-ir neurones were only identified in the mouse striatum after combined administration of a dopaminergic neurotoxin [1-methyl-4-phenyl-1,2,5,6-tetrahydropyridine (MPTP)] with the mitochondrial inhibitor 3-nitropropionic acid

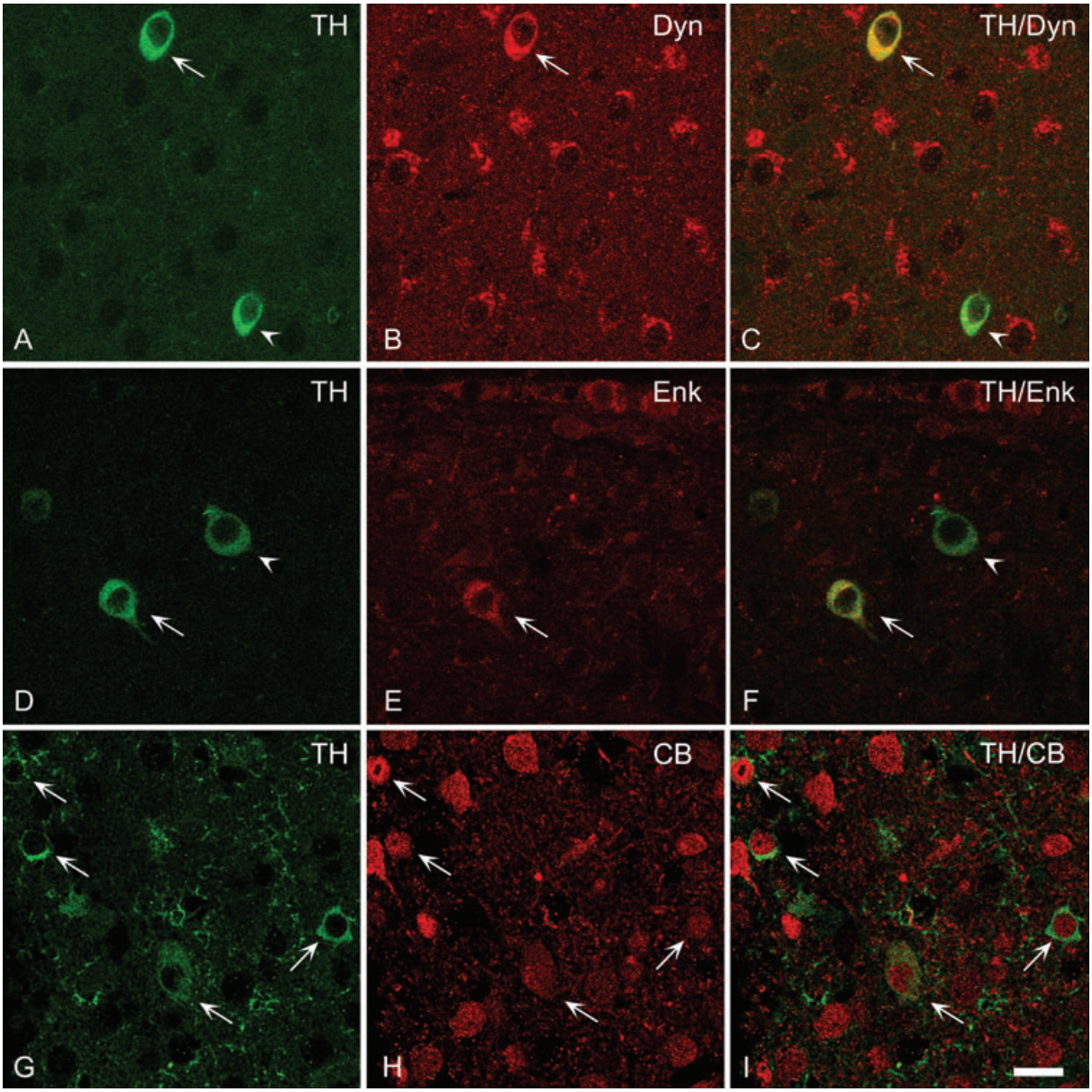

FIG. 6. Expression of striatal projection neurone markers dynorphin (Dyn), enkephalin (Enk) and calbindin (CB) in TH-ir neurones in the mouse striatum following 6-OHDA lesion and L-DOPA treatment. Confocal laser photomicrographs of striatal sections from mice killed at 7 weeks after unilateral 6-OHDA injection and treated with daily L-DOPA treatment for the last 3 weeks. Sections were analysed by double immunohistochemistry with antibodies to TH and either Dyn (A–C), Enk (D and E) or CB (F–I) antibodies. Arrows indicate double-labelled neurones and arrowheads indicate single-labelled neurones. Scale bars: 15 μm (A–F); 17 μm (G–I).

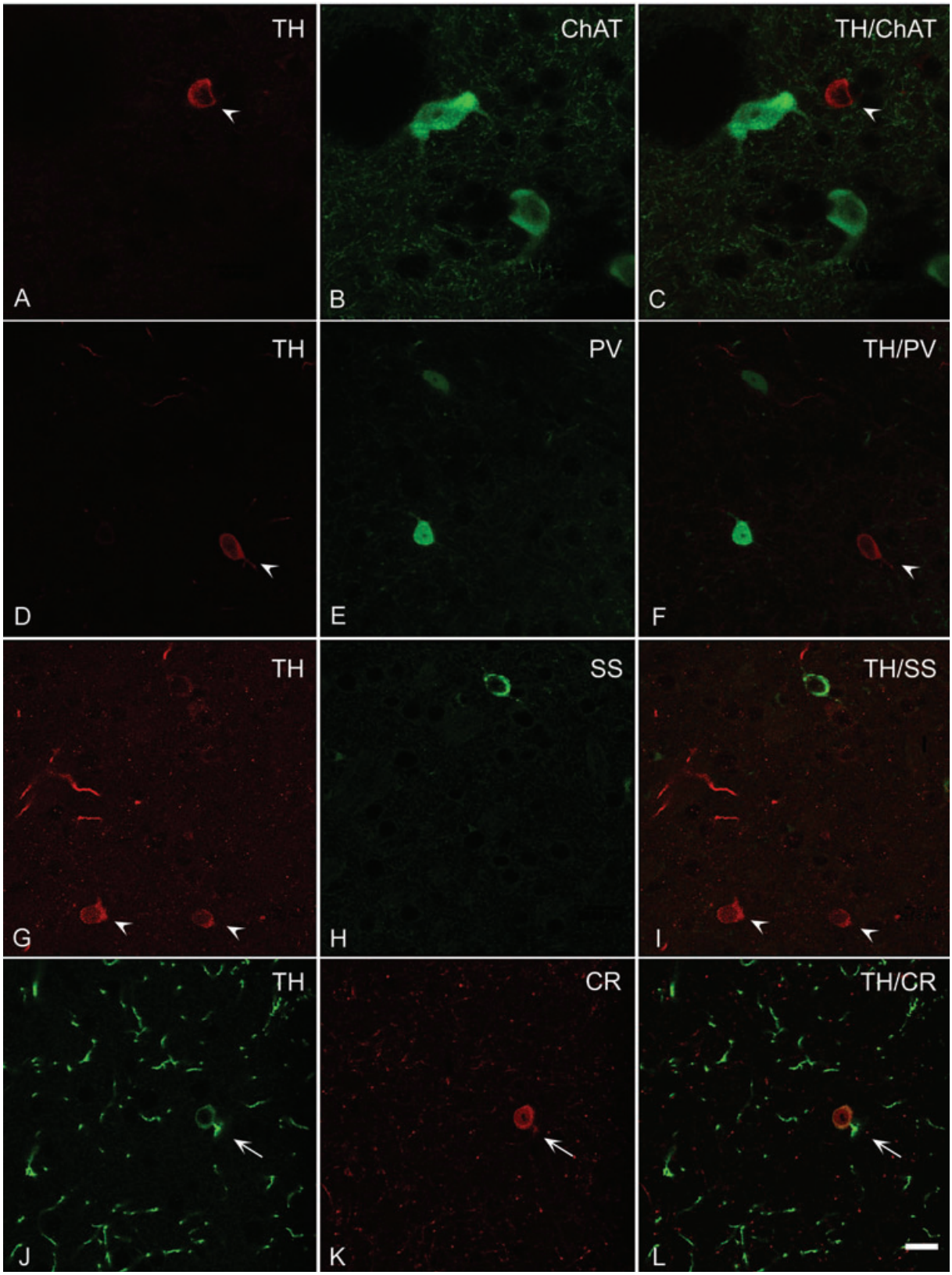

FIG. 7. Expression of markers for striatal interneurones in TH-ir neurones in the mouse striatum following 6-OHDA lesion and L-DOPA treatment. Confocal laser photomicrographs of striatal sections showing immunofluorescence staining with TH antibody in combination with antibodies for choline acetyltransferase (ChAT) (A–C), parvalbumin (PV) (D–F), somatostatin (SS) (G–I) or calretinin (CR) (J–L). Colocalization with TH was only observed for CR (L). Arrows indicate double-labelled neurones and arrowheads indicate single-labelled neurones. All sections are from animals killed at 7 weeks after 6-OHDA lesion, with L-DOPA treatment for the last 3 weeks. Scale bars: 12 μm (A–C); 15 μm (D–F and J–L); 17 μm (G–I).

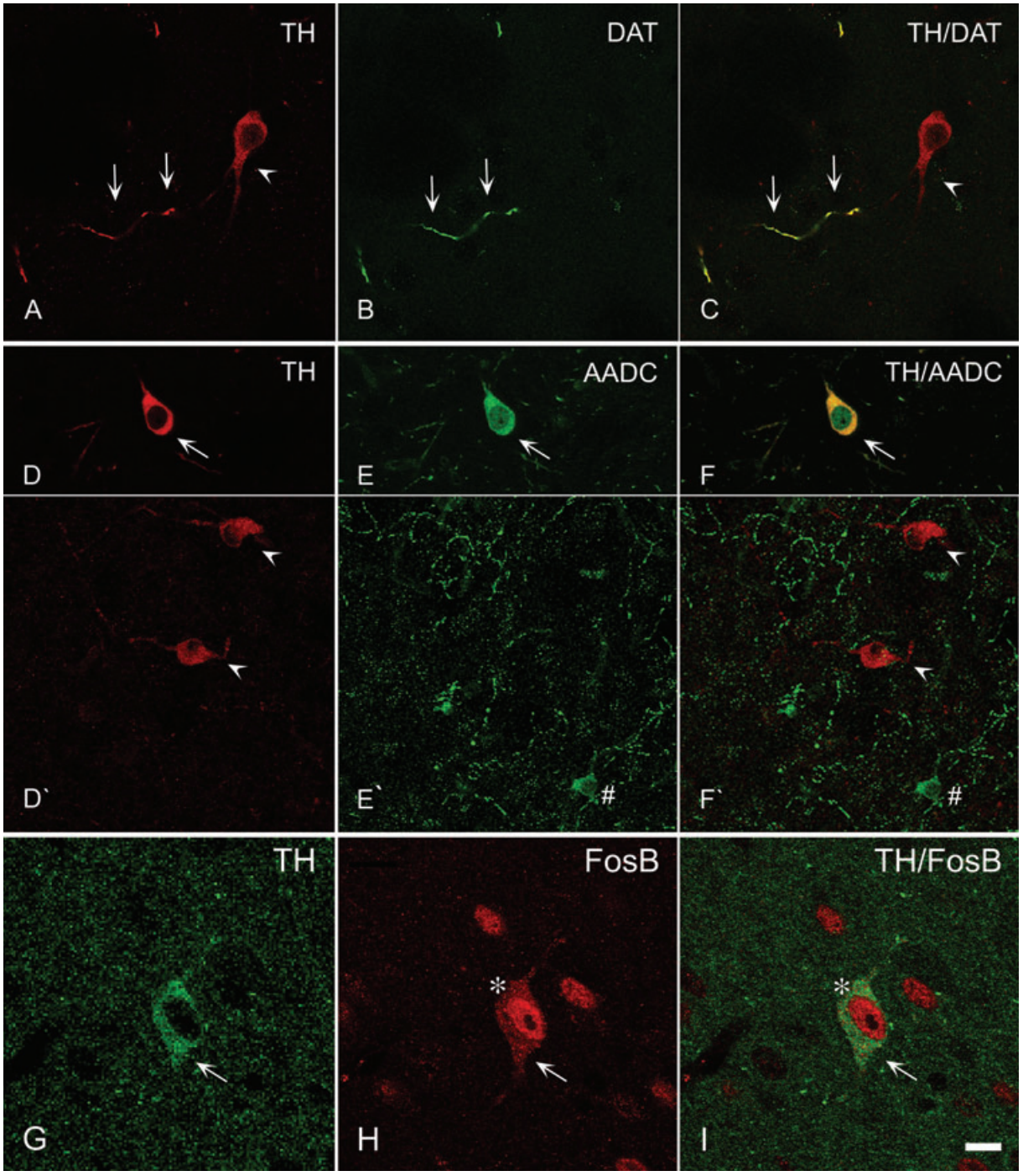

FIG. 8. Expression of dopaminergic markers and the neuronal activation marker, FosB, in striatal TH-ir neurones following 6-OHDA lesion and L-DOPA treatment. Confocal laser photomicrographs of striatal sections from mice killed at 7 weeks after 6-OHDA lesions, with L-DOPA treatment for the last 3 weeks. Immunofluorescence staining with a TH antibody in combination with antibodies to DAT (A–C), AADC (D–F′) or FosB (G–I). Colocalization with TH is marked with arrows; lack of colocalization is indicated with arrowheads. DAT was only colocalized with TH in the spared dopaminergic fibres (C) shown in yellow. AADC and FosB colocalized with TH (F and I). Note the unusual expression of FosB in the cytoplasm of TH-ir neurones (H and I, marked with asterisks). (D′–F′) An example of TH-ir neurones that do not contain AADC. #Example of AADC+/TH-neurones. Scale bars: 15 μm (A–C); 20 μm (D–F); 10 μm (G–I).

(Nakahara *et al.*, 2001), in DAT knock-out mice (Jaber *et al.*, 1999) or during development (Komori *et al.*, 1991).

In our study, TH-ir neurones appeared in the striatum soon after 6-lesion (3 days), in agreement with data from other studies in rodents (Meredith *et al.*, 1999; Nakahara *et al.*, 2001; Jollivet *et al.*, 2004). However, their density in the striatum decreased to 10% of the initial values by 7 weeks post-lesion, with a concomitant decrease in the intensity of labelling in the majority of neurones. This is in agreement with results obtained previously in the rat after 6-OHDA (Meredith *et al.*, 1999) and in mouse striatum after MPTP and 3-nitropropionic acid (Nakahara *et al.*, 2001). However, other studies in rats reported either no change with time (Lopez-Real *et al.*, 2003) or an increase in

the number of TH-ir neurones with time after the lesion (Jollivet *et al.*, 2004). These differences with respect to the density of TH-ir neurones after dopamine depletion could be due to differences in the lesion (injection of 6-OHDA into the striatum vs. medial forebrain bundle), intensity of the lesion or the species examined (rat vs. mouse).

In agreement with previous reports, we did not detect TH-ir neurones in the non-lesioned striatum (Betarbet *et al.*, 1997; Meredith *et al.*, 1999). We cannot exclude the possibility that TH-ir neurones were masked by the dense TH-ir fibres in the intact mouse striatum. However, we think that this is unlikely as we expect that confocal microscopy should have revealed soma staining as it was described in normal primate and human striatum (Betarbet *et al.*, 1997; Cossette *et al.*, 2005a; Weihe *et al.*, 2006; Huot *et al.*, 2007). It has been reported that a few sparsely scattered cells in the striatum of normal mice express TH mRNA without detectable levels of TH protein (Jaber *et al.*, 1999; Baker *et al.*, 2003). It is possible that after dopaminergic denervation these neurones begin to express detectable amounts of TH protein. Further studies are needed to address this possibility.

Interestingly, L-DOPA treatment markedly increased the intensity of TH immunostaining and the labelling of dendrites of TH-ir striatal neurones, producing a significant increase in their cellular density to above the values detected at 0.5 week after the lesion. An increase in the number of TH-ir neurones after L-DOPA treatment has been described previously in rats (Jollivet *et al.*, 2004), as well as in MPTP-treated monkeys receiving carotid body grafts in the putamen (San Sebastian *et al.*, 2007). In the lesioned mice treated with saline instead of L-DOPA, striatal TH-ir neurones were only detected in the ventral striatum or close to the remaining dopaminergic fibres after the lesion. Whereas TH-ir neurones in the L-DOPA-treated animals were mostly observed in the dorsal and dorsolateral striatum near spared dopamine fibres, almost no TH cells were found in striatal areas with a complete absence of TH fibres. This distribution of TH-ir neurones is in agreement with previous results in the rat (Meredith *et al.*, 1999; Mura *et al.*, 2000; Nakahara *et al.*, 2001; Jollivet *et al.*, 2004). Taken together, these results indicate that the neuronal expression of TH in the striatum caused by the 6-OHDA lesion is not maintained without residual innervation from the substantia nigra or additional dopaminergic stimulation, such as that provided by L-DOPA treatment. Therefore, the TH expression in these cells seems to be regulated by the local concentration of dopamine.

Tyrosine hydroxylase is an enzyme that is controlled by almost all documented forms of physiological regulation. It is responsible for a critical step in the synthesis of dopamine, norepinephrine and epinephrine, which occurs in a wide variety of different tissues serving different functions (Kumer & Vrana, 1996). Two possible hypotheses have been proposed for the induction of TH expression in striatal neurones: (i) rapid changes in dopamine content (Meredith *et al.*, 1999) and (ii) the expression of growth factors after the lesion (Daadi & Weiss, 1999; Palfi *et al.*, 2002; Jollivet *et al.*, 2004). The appearance of TH-ir neurones after dopamine depletion in our experiments could be explained by both effects, by the rapid changes in dopamine content in the striatum produced by deafferentation and/or by trophic factors produced by glial cells that proliferate after the lesion. Similarly, the preservation and further increase of TH immunoreactivity in striatal neurones produced by L-DOPA treatment could be a consequence of the repetitive fluctuation in striatal dopamine levels. Following denervation, striatal DA levels are very low and the repeated L-DOPA treatment presumably creates fluctuating striatal DA content throughout the duration of the treatment. The fact that TH neurones are most frequently found close to spared dopaminergic terminals further supports their dopamine dependency, as these terminals are the most likely site of conversion of L-DOPA to dopamine. Alternatively, the appearance of TH neurones may be induced by the trophic effects of L-DOPA and dopamine (Du & Iacovitti, 1995) or by the L-DOPA-induced increase in glutamate release in the striatum after 6-OHDA administration (Misu *et al.*, 1996). Such a role for glutamate in the induction of striatal TH-ir neurones has been suggested previously (Betarbet & Greenamyre, 1999). It is not clear why denervation induces TH expression in only a small fraction of striatal neurones and the functional consequence of this phenotype induction is unknown.

BrdU incorporation and the molecular phenotype of TH-ir neurones

Despite various reports favouring the immaturity of striatal TH-ir neurones based on their low content of the ageing-related pigment lipofuscin (Betarbet *et al.*, 1997; Cossette *et al.*, 2005b; Tande *et al.*, 2006), we did not detect any newly generated TH-ir cells in the striatum using incorporation of BrdU or by doublecortin and nestin immunohistochemistry. This suggests that TH-ir neurones in the mouse striatum arise through a change in the phenotype of neurones already present in the striatum before 6-OHDA administration, as shown previously in MPTP-treated macaques (Tande *et al.*, 2006).

The major finding of our molecular characterization of the TH-ir neurones is their colocalization with the neuropeptides enkephalin and dynorphin, which has not been reported previously in any of the species studied. We found that TH expression occurred mainly in the projection neurones of the direct and indirect pathway, establishing the major phenotype of these striatal TH-ir neurones. These results are in agreement with previous observations in rodents (Tashiro *et al.*, 1989; Meredith *et al.*, 1999; Nakahara *et al.*, 2001), which indicated that TH-ir neurones are projection neurones based on their morphology as observed by optic and electron microscopy. Interestingly, dendritic spines were not evident in the majority of the TH-ir neurones observed in our study, although dendritic spines have been reported on these neurones previously (Tashiro *et al.*, 1989; Nakahara *et al.*, 2001). In our study, dendritic spines were only observed on a small number of neurones with well-marked dendritic trees and these neurones were always located close to the spared dopaminergic terminals. This indicates that the absence of dendritic spines is probably due to their retraction after striatal denervation (Meredith *et al.*, 1995; Nitsch & Riesenberg, 1995; Ingham *et al.*, 1998; Day *et al.*, 2006) or, alternatively, it could be due to the lack of TH expression in these particular areas of the neurone preventing their visualization.

Only 1% of TH-ir neurones in the lesioned mouse striatum expressed calretinin, identifying them as interneurones. This is in agreement with data obtained in the monkey striatum (Tande *et al.*, 2006). In the human striatum, a higher percentage of TH-ir neurones (30%) was found to express calretinin (Cossette *et al.*, 2005b). TH immunoreactivity in the primate striatum was localized in striatal interneurones (Ingham *et al.*, 1998; Tande *et al.*, 2006; San Sebastian *et al.*, 2007), contrasting with our findings in the mouse; however, these authors did not study localization of TH with specific projection neurone markers. This discrepancy could be due to a higher ratio of projection neurones to interneurones in the rodent compared with the primate striatum (Graveland & DiFiglia, 1985), as well as the higher proportion of calretinin neurones in the human striatum (Wu & Parent, 2000).

Functional considerations of TH-ir neurones in the dopamine-depleted striatum

We did not detect any DAT-ir cells in the mice striatum, in contrast with previous studies of monkey striatum (Betarbet *et al.*, 1997; Porritt *et al.*, 2000; Cossette *et al.*, 2005a,b; Tande *et al.*, 2006). We also describe two other differences between mouse striatum and primate striatum: (i) striatal TH-ir neurones are not found in naive mice (Jaber *et al.*, 1999; Baker *et al.*, 2003) but are observed in naive primates (Dubach *et al.*, 1987; Betarbet *et al.*, 1997; Tande *et al.*, 2006) and (ii) most TH-ir neurones are projection neurones in 6-OHDA-lesioned mice but have been described as interneurones in the striatum of MPTP-treated monkey (Tande *et al.*, 2006; San Sebastian *et al.*, 2007).

Our findings indicate that about half of the striatal TH-ir neurones in the mouse striatum also express AADC, the final enzyme in the dopamine synthesis cascade. This colocalization of TH with AADC in the rat striatum has been described by others (Lopez-Real *et al.*, 2003) and enables the neurones to synthesize dopamine. The other half of striatal TH-ir neurones do not contain AADC. Neurones that express TH but not AADC have also been described in the hypothalamus, thalamus, cerebral cortex and spinal cord (Weihe *et al.*, 2006). These neurones appear to produce and store L-DOPA and therefore were classified as 'dopaergic catecholaminergic neurones' (Weihe *et al.*, 2006). Therefore, it appears that L-DOPA can behave as a neurotransmitter in the central nervous system (Misu *et al.*, 1996). It is possible, as mentioned in Lopez-Real *et al.* (2003), that these TH neurones also express AADC below immunohistochemically detectable levels and therefore contribute to dopamine production (Bjorklund & Dunnett, 2007). Alternatively, the presence of neurones in the rodent striatum expressing individual and complementary enzymes for dopamine synthesis (TH alone and AADC alone) presents the possibility that these neurones could work together to produce dopamine (Ugrumov *et al.*, 2004). Thus, the L-DOPA produced in TH neurones could be released, taken up by AADC neurones (Ugrumov *et al.*, 2004) and converted into dopamine. Although the amount of dopamine synthesized in this way may be low, the marked reduction in dopamine transport that accompanies the induction of the TH phenotype should favour long-distance diffusion and the existence of supersensitive dopamine receptors in the denervated striatum should increase the effect of small amounts of dopamine (Pavon *et al.*, 2006). Independently, L-DOPA can also be taken up and converted to dopamine by serotonergic terminals as recently shown by Carta *et al.* (2007).

To address the important question of whether TH-ir neurones are active in the lesioned striatum, we studied FosB expression after dopaminergic stimulation. Dopamine derived from exogenously administered L-DOPA can stimulate dopamine receptors on striatal TH neurones and induce FosB expression, which was detected in all TH-ir neurones following L-DOPA treatment. The regulatory region of the TH gene bears an activator protein-1 binding site, where FosB might bind as a dimer with another member of the leucine zipper family (Trocme *et al.*, 1998; Lewis-Tuffin *et al.*, 2004). Thus, it is conceivable that the induction of FosB is involved in maintenance of the TH phenotype, although there is currently no evidence to support this hypothesis.

Although the effect of inducing the TH phenotype in presumed projection neurones of denervated mouse striatum is not known, it is possible that it serves as a compensatory mechanism that increases dopamine content, alleviating the motor effects caused by the dopaminergic lesion (Bjorklund & Dunnett, 2007). As we show here with FosB expression, these cells are active and respond to L-DOPA. It is possible, as mentioned above, that striatal TH-ir cells produce dopamine. Although this would produce only very low levels of dopamine, it has been shown that very small numbers of dopamine-producing cells can reduce parkinsonian symptoms in denervated rats receiving carotid body grafts into the striatum (Espejo *et al.*, 1998). Similarly, carotid body grafts in MPTP-treated monkeys increased the number of striatal TH-ir neurones and this increase was associated with long-term motor recovery from their parkinsonian state (San Sebastian *et al.*, 2007). It is therefore possible that the induction of TH expression that we observed following L-DOPA treatment in denervated mice could help to alleviate parkinsonian symptoms.

In summary, the results reported here establish for the first time that TH is expressed mainly in a subset of projection neurones in the mouse striatum following 6-OHDA lesion. This expression decreases with time but can be maintained and potentiated by L-DOPA. In addition, we demonstrate that these neurones respond to L-DOPA stimulation. The shift of a small number of striatal projection neurones to a TH phenotype may help to counteract the motor consequences of the lesion. If this is the case, promoting the phenotypic change should be beneficial in Parkinson's disease, particularly during the early stages when dopamine denervation is incomplete. It will be important to determine the exact function of these neurones and the cellular mechanisms responsible for this phenotype induction. Understanding these mechanisms may suggest new avenues for the treatment of Parkinson's disease.

Supplementary material

The following supplementary material may be found on
http://www.blackwell-synergy.com

Fig. S1. Absence of TH-ir neurones in the unlesioned striatum.

Please note: Blackwell Publishing are not responsible for the content or functionality of any supplementary materials supplied by the authors. Any queries (other than missing material) should be directed to the correspondence author for the article.

Acknowledgements

This research was supported by grants from the Spanish Ministerio de Ciencia y Tecnología (SAF2003-4864, GEN2003-C06-02/NAC) and the Spanish Ministerio de Sanidad y Consumo, Fondo de Investigación Sanitaria (PI0710B, RTA RD06/0001, PNSD, CIBERNED). The authors would like to thank Dr J. DeFelipe for the use of the Neurolucida system and Carmen Hernández for her excellent assistance with confocal microscopy. Special thanks to Dr A. Del Arco for his constructive and helpful comments on the manuscript and to A. Mendialdua for the help with TH/FosB immunohistochemistry.

Abbreviations

AADC, aromatic-L-amino acid decarboxylase; BrdU, 5-bromo-2-deoxyuridine; DAT, dopamine transporter; ir, immunoreactive; L-DOPA, L-3,4-dihydroxyphenylalanine; MPTP, 1-methyl-4-phenyl-1,2,5,6-tetrahydropyridine; 6-OHDA, 6-hydroxydopamine; TH, tyrosine hydroxylase.

References

Andersson, M., Hilbertson, A. & Cenci, M.A. (1999) Striatal fosB expression is causally linked with l-DOPA-induced abnormal involuntary movements and the associated upregulation of striatal prodynorphin mRNA in a rat model of Parkinson's disease. *Neurobiol. Dis.*, **6**, 461–474.

Baker, H., Kobayashi, K., Okano, H. & Saino-Saito, S. (2003) Cortical and striatal expression of tyrosine hydroxylase mRNA in neonatal and adult mice. *Cell Mol. Neurobiol.*, **23**, 507–518.

Bedard, A., Cossette, M., Levesque, M. & Parent, A. (2002) Proliferating cells can differentiate into neurons in the striatum of normal adult monkey. *Neurosci. Lett.*, **328**, 213–216.

Betarbet, R. & Greenamyre, J.T. (1999) Differential expression of glutamate receptors by the dopaminergic neurons of the primate striatum. *Exp. Neurol.*, **159**, 401–408.

Betarbet, R., Turner, R., Chockkan, V., Delong, M.R., Allers, K.A., Walters, J., Levey, A.I. & Greenamyre, J.T. (1997) Dopaminergic neurons intrinsic to the primate striatum. *J. Neurosci.*, **17**, 6761–6768.

Bjorklund, A. & Dunnett, S.B. (2007) Dopamine neuron systems in the brain: an update. *Trends Neurosci.*, **30**, 194–202.

Breese, G.R. & Traylor, T.D. (1971) Depletion of brain noradrenaline and dopamine by 6-hydroxydopamine. *Br. J. Pharmacol.*, **42**, 88–99.

Carta, M., Carlsson, T., Kirik, D. & Björklund, A. (2007) Dopamine released from 5-HT terminals is the cause of L-DOPA-induced dyskinesia in parkinsonian rats. *Brain*, **130**, 1819–1833.

Chang, H.T., Wilson, C.J. & Kitai, S.T. (1982) A Golgi study of rat neostriatal neurons: light microscopic analysis. *J. Comp. Neurol.*, **208**, 107–126.

Cossette, M., Parent, A. & Levesque, D. (2004) Tyrosine hydroxylase-positive neurons intrinsic to the human striatum express the transcription factor Nurr1. *Eur. J. Neurosci.*, **20**, 2089–2095.

Cossette, M., Lecomte, F. & Parent, A. (2005a) Morphology and distribution of dopaminergic neurons intrinsic to the human striatum. *J. Chem. Neuroanat.*, **29**, 1–11.

Cossette, M., Levesque, D. & Parent, A. (2005b) Neurochemical characterization of dopaminergic neurons in human striatum. *Parkinsonism Relat. Disord.*, **11**, 277–286.

Daadi, M.M. & Weiss, S. (1999) Generation of tyrosine hydroxylase-producing neurons from precursors of the embryonic and adult forebrain. *J. Neurosci.*, **19**, 4484–4497.

Day, M., Wang, Z., Ding, J., An, X., Ingham, C.A., Shering, A.F., Wokosin, D., Ilijic, E., Sun, Z., Sampson, A.R., Mugnaini, E., Deutch, A.Y., Sesack, S.R., Arbuthnott, G.W. & Surmeier, D.J. (2006) Selective elimination of glutamatergic synapses on striatopallidal neurons in Parkinson disease models. *Nat. Neurosci.*, **9**, 251–259.

DiFiglia, M., Pasik, P. & Pasik, T. (1976) A Golgi study of neuronal types in the neostriatum of monkeys. *Brain Res.*, **114**, 245–256.

Du, X. & Iacovitti, L. (1995) Synergy between growth factors and transmitters required for catecholamine differentiation in brain neurons. *J. Neurosci.*, **15**, 5420–5427.

Dubach, M., Schmidt, R., Kunkel, D., Bowden, D.M., Martin, R. & German, D.C. (1987) Primate neostriatal neurons containing tyrosine hydroxylase: immunohistochemical evidence. *Neurosci. Lett.*, **75**, 205–210.

Espejo, E.F., Montoro, R.J., Armengol, J.A. & Lopez-Barneo, J. (1998) Cellular and functional recovery of Parkinsonian rats after intrastriatal transplantation of carotid body cell aggregates. *Neuron*, **20**, 197–206.

Gerfen, C.R., Baimbridge, K.G. & Miller, J.J. (1985) The neostriatal mosaic: compartmental distribution of calcium-binding protein and parvalbumin in the basal ganglia of the rat and monkey. *Proc. Natl Acad. Sci. U.S.A.*, **82**, 8780–8784.

Granado, N., Escobedo, I., O'Shea, E., Colado, M.I. & Moratalla, R. (2008) Early loss of dopaminergic terminals in striosomes after MDMA administration to mice. *Synapse*, **62**, 80–84.

Grande, C., Zhu, H., Martin, A.B., Lee, M., Ortiz, O., Hiroi, N. & Moratalla, R. (2004) Chronic treatment with atypical neuroleptics induces striosomal FosB/DeltaFosB expression in rats. *Biol. Psychiat.*, **55**, 457–463.

Graveland, G.A. & DiFiglia, M. (1985) The frequency and distribution of medium-sized neurons with indented nuclei in the primate and rodent neostriatum. *Brain Res.*, **327**, 307–311.

Huot, P. & Parent, A. (2007) Dopaminergic neurons intrinsic to the striatum. *J. Neurochem.*, **101**, 1441–1447.

Huot, P., Levesque, M. & Parent, A. (2007) The fate of striatal dopaminergic neurons in Parkinson's disease and Huntington's chorea. *Brain*, **130**, 222–232.

Ingham, C.A., Hood, S.H., Taggart, P. & Arbuthnott, G.W. (1998) Plasticity of synapses in the rat neostriatum after unilateral lesion of the nigrostriatal dopaminergic pathway. *J. Neurosci.*, **18**, 4732–4743.

Jaber, M., Dumartin, B., Sagne, C., Haycock, J.W., Roubert, C., Giros, B., Bloch, B. & Caron, M.G. (1999) Differential regulation of tyrosine hydroxylase in the basal ganglia of mice lacking the dopamine transporter. *Eur. J. Neurosci.*, **11**, 3499–3511.

Jollivet, C., Montero-Menei, C.N., Venier-Julienne, M.C., Sapin, A., Benoit, J.P. & Menei, P. (2004) Striatal tyrosine hydroxylase immunoreactive neurons are induced by L-dihydroxyphenylalanine and nerve growth factor treatment in 6-hydroxydopamine lesioned rats. *Neurosci. Lett.*, **362**, 79–82.

Kawaguchi, Y., Wilson, C.J. & Emson, P.C. (1990) Projection subtypes of rat neostriatal matrix cells revealed by intracellular injection of biocytin. *J. Neurosci.*, **10**, 3421–3438.

Kawaguchi, Y., Wilson, C.J., Augood, S.J. & Emson, P.C. (1995) Striatal interneurones: chemical, physiological and morphological characterization. *Trends Neurosci.*, **18**, 527–535.

Komori, K., Sakai, M., Karasawa, N., Yamada, K. & Nagatsu, I. (1991) Evidence for transient expression of tyrosine hydroxylase immunoreactivity in the mouse striatum and the effect of colchicine. *Acta Histochem. Cytochem.*, **24**, 223–231.

Kumer, S.C. & Vrana, K.E. (1996) Intricate regulation of tyrosine hydroxylase activity and gene expression. *J. Neurochem.*, **67**, 443–462.

Lewis-Tuffin, L.J., Quinn, P.G. & Chikaraishi, D.M. (2004) Tyrosine hydroxylase transcription depends primarily on cAMP response element activity, regardless of the type of inducing stimulus. *Mol. Cell Neurosci.*, **25**, 536–547.

Lopez-Real, A., Rodriguez-Pallares, J., Guerra, M.J. & Labandeira-Garcia, J.L. (2003) Localization and functional significance of striatal neurons immunoreactive to aromatic L-amino acid decarboxylase or tyrosine hydroxylase in rat Parkinsonian models. *Brain Res.*, **969**, 135–146.

Lundblad, M., Picconi, B., Lindgren, H. & Cenci, M.A. (2004) A model of L-DOPA-induced dyskinesia in 6-hydroxydopamine lesioned mice: relation to motor and cellular parameters of nigrostriatal function. *Neurobiol. Dis.*, **16**, 110–123.

Mazloom, M. & Smith, Y. (2006) Synaptic microcircuitry of tyrosine hydroxylase-containing neurons and terminals in the striatum of 1-methyl-4-phenyl-1,2,3,6-tetrahydropyridine-treated monkeys. *J. Comp. Neurol.*, **495**, 453–469.

McManus, M.F., Chen, L.C., Vallejo, I. & Vallejo, M. (1999) Astroglial differentiation of cortical precursor cells triggered by activation of the cAMP-dependent signaling pathway. *J. Neurosci.*, **19**, 9004–9015.

Mercugliano, M., Soghomonian, J.J., Qin, Y., Nguyen, H.Q., Feldblum, S., Erlander, M.G., Tobin, A.J. & Chesselet, M.F. (1992) Comparative distribution of messenger RNAs encoding glutamic acid decarboxylases (Mr 65,000 and Mr 67,000) in the basal ganglia of the rat. *J. Comp. Neurol.*, **318**, 245–254.

Meredith, G.E., Ypma, P. & Zahm, D.S. (1995) Effects of dopamine depletion on the morphology of medium spiny neurons in the shell and core of the rat nucleus accumbens. *J. Neurosci.*, **15**, 3808–3820.

Meredith, G.E., Farrell, T., Kellaghan, P., Tan, Y., Zahm, D.S. & Totterdell, S. (1999) Immunocytochemical characterization of catecholaminergic neurons in the rat striatum following dopamine-depleting lesions. *Eur. J. Neurosci.*, **11**, 3585–3596.

Milstein, C. & Cuello, A.C. (1983) Hybrid hybridomas and their use in immunohistochemistry. *Nature*, **305**, 537–540.

Misu, Y., Goshima, Y., Ueda, H. & Okamura, H. (1996) Neurobiology of L-DOPAergic systems. *Prog. Neurobiol.*, **49**, 415–454.

Moratalla, R., Elibol, B., Vallejo, M. & Graybiel, A.M. (1996) Network-level changes in expression of inducible Fos-Jun proteins in the striatum during chronic cocaine treatment and withdrawal. *Neuron*, **17**, 147–156.

Mura, A., Jackson, D., Manley, M.S., Young, S.J. & Groves, P.M. (1995) Aromatic L-amino acid decarboxylase immunoreactive cells in the rat striatum: a possible site for the conversion of exogenous L-DOPA to dopamine. *Brain Res.*, **704**, 51–60.

Mura, A., Feldon, J. & Mintz, M. (2000) The expression of the calcium binding protein calretinin in the rat striatum: effects of dopamine depletion and L-DOPA treatment. *Exp. Neurol.*, **164**, 322–332.

Nakahara, T., Yamamoto, T., Endo, K. & Kayama, H. (2001) Neuronal ectopic expression of tyrosine hydroxylase in the mouse striatum by combined administration of 1-methyl-4-phenyl-1,2,3,6-tetrahydropyridine and 3-nitropropionic acid. *Neuroscience*, **108**, 601–610.

Nitsch, C. & Riesenberg, R. (1995) Synaptic reorganisation in the rat striatum after dopaminergic deafferentation: an ultrastructural study using glutamate decarboxylase immunocytochemistry. *Synapse*, **19**, 247–263.

Palfi, S., Leventhal, L., Chu, Y., Ma, S.Y., Emborg, M., Bakay, R., Deglon, N., Hantraye, P., Aebischer, P. & Kordower, J.H. (2002) Lentivirally delivered glial cell line-derived neurotrophic factor increases the number of striatal dopaminergic neurons in primate models of nigrostriatal degeneration. *J. Neurosci.*, **22**, 4942–4954.

Pavon, N., Martin, A.B., Mendialdua, A. & Moratalla, R. (2006) ERK phosphorylation and FosB expression are associated with L-DOPA-induced dyskinesia in hemiparkinsonian mice. *Biol. Psychiat.*, **59**, 64–74.

Paxinos, G. & Franklin, K.B.J. (2004) *The Mouse Brain in Stereotaxic Coordinates*. Elsevier Science, USA.

Porritt, M.J., Batchelor, P.E., Hughes, A.J., Kalnins, R., Donnan, G.A. & Howells, D.W. (2000) New dopaminergic neurons in Parkinson's disease striatum. *Lancet*, **356**, 44–45.

Rivera, A., Alberti, I., Martin, A.B., Narvaez, J.A., de la Calle, A. & Moratalla, R. (2002) Molecular phenotype of rat striatal neurons expressing the dopamine D5 receptor subtype. *Eur. J. Neurosci.*, **16**, 2049–2058.

San Sebastian, W., Guillen, J., Manrique, M., Belzunegui, S., Ciordia, E., Izal-Azcarate, A., Garrido-Gil, P., Vazquez-Claverie, M. & Luquin, M.R. (2007) Modification of the number and phenotype of striatal dopaminergic cells by carotid body graft. *Brain*, **130**, 1306–1316.

Tande, D., Hoglinger, G., Debeir, T., Freundlieb, N., Hirsch, E.C. & Francois, C. (2006) New striatal dopamine neurons in MPTP-treated macaques result from a phenotypic shift and not neurogenesis. *Brain*, **129**, 1194–1200.

Tashiro, Y., Sugimoto, T., Hattori, T., Uemura, Y., Nagatsu, I., Kikuchi, H. & Mizuno, N. (1989) Tyrosine hydroxylase-like immunoreactive neurons in the striatum of the rat. *Neurosci. Lett.*, **97**, 6–10.

Trocme, C., Sarkis, C., Hermel, J.M., Duchateau, R., Harrison, S., Simonneau, M., Al-Shawi, R. & Mallet, J. (1998) CRE and TRE sequences of the rat tyrosine hydroxylase promoter are required for TH basal expression in adult mice but not in the embryo. *Eur. J. Neurosci.*, **10**, 508–521.

Ugrumov, M.V., Melnikova, V.I., Lavrentyeva, A.V., Kudrin, V.S. & Rayevsky, K.S. (2004) Dopamine synthesis by non-dopaminergic neurons expressing individual complementary enzymes of the dopamine synthetic pathway in the arcuate nucleus of fetal rats. *Neuroscience*, **124**, 629–635.

Weihe, E., Depboylu, C., Schutz, B., Schafer, M.K. & Eiden, L.E. (2006) Three types of tyrosine hydroxylase-positive CNS neurons distinguished by Dopa decarboxylase and VMAT2 co-expression. *Cell Mol. Neurobiol.*, **26**, 657–676.

Wu, Y. & Parent, A. (2000) Striatal interneurons expressing calretinin, parvalbumin or NADPH-diaphorase: a comparative study in the rat, monkey and human. *Brain Res.*, **863**, 182–191.